01 Jan 1973

Turbulence Measurements with a Sampling Laser-Doppler Velocimeter

P. D. Iten

TURBULENCE MEASUREMENTS WITH A SAMPLING LASER DOPPLER VELOCIMETER

P. D. Iten
Brown Boveri Research Center
CH-5401 Baden, Switzerland

ABSTRACT

A novel sampling signal processor overcomes the difficulties encountered with frequency trackers in the investigation of unseeded highly turbulent flows. This sampling system consists essentially of a swept filter, e.g. a standard RF-spectrum analyzer, a digital data memory and a storage oscilloscope. It is able to determine first-order statistical averages of turbulent flows with high fluctuation frequencies and amplitudes even at very low scattering particle concentrations. Since the velocity samples are not statistically independent of the velocity, the sampled velocity data has to be corrected in order to obtain unbiased statistical averages. A theoretical analysis and experimental investigations of the system and its application are given.

INTRODUCTION

The output signal of a laser Doppler velocimeter (LDV) is produced by light pulses scattered by small particles during their transit time through the probe volume. Therefore, a Doppler signal is not a continuous wave but rather consists of randomly occurring Doppler bursts. Each one of these bursts represents a sample of the velocity function to be measured. The mean time interval between such velocity samples determines the mean sample rate which thus depends on the product of velocity and particle concentration. In the case of time dependent flow, e.g. turbulence phenomena, this sample rate, as stated by the sampling theorem, gives the basic limit for the temporal resolution with which a velocity-time function can be reconstructed. This limitation - discontinuous information flow due to finite particle concentration - is given by information theory (1) and holds for any LDV.

In laser Doppler anemometry one therefore usually seeds the flow with artificial scattering particles in order to increase the sample rate and obtain an information flow as continuous as possible. In this case the temporal resolution of the LDV is limited only by the response time of the electronic signal processor. If seeding is not possible, additional limitations, due to specific design principles of the different classes of signal processing systems, are imposed on the temporal fluctuations of the flow velocity.

In this paper the influence of the scattering particle concentration on the temporal resolution and the measurement accuracy is discussed. Limitations of frequency tracking systems for the investigations of turbulent flows are shown and compared with two sampling techniques, the gated zero crossing detector (2) and a novel sampling signal processor for spectrum analyzers (3). The latter system will be described in detail and experimental results of measurements in an air jet, a turbulent water pipe, and in Karman vortices will be given.

THE DOPPLER SIGNAL

For the present investigations the flow velocity $\vec{u}(t)$ is assumed to be a stationary random process (Figure 1). The corresponding instantaneous Doppler frequency, $\nu(t)$, is related to the flow velocity, $\vec{u}(t)$, by the following well known relation:

$$\nu(t) = \vec{k} \cdot \vec{u}(t) = |\vec{k}| \; u_k(t) \; , \qquad (1)$$

where $u_k(t)$ denotes the component of the velocity vector, $\vec{u}(t)$, in the direction of the sensitivity vector, $\vec{k}$, and the system constant, $|k|$, is given by

$$|\vec{k}| = \frac{2 \sin \chi}{\lambda} \; , \qquad (2)$$

where 2χ and λ are the measurement angle (4) and the laser wavelength, respectively.

Hence, $\nu(t)$ in Equation 1 is a measure for the velocity component, $u_k(t)$, in the direction of the sensitivity vector, $\vec{k}$. Since only one-dimensional considerations are made in this paper, for convenience, the sensitivity vector, k, is assumed to be parallel to the principal flow axis, and the index, k, of the velocity component, $u_k(t)$ is omitted: $u_k(t) \rightarrow u(t)$.

An individual scattering particle may be considered as producing a typical signal (ac-term) like

$$i_n(t) = a_n(t) \cos[2\pi\nu(t) \cdot (t - t_n)] \; , \qquad (3)$$

where the envelope $a_n(t)$ is a Gaussian and depends on the Gaussian intensity distribution within the probe volume along the trajectory of the n-th particle (2). t_n is the time of occurrence of the n-th particle, i.e. the time when the signal envelope, $a_n(t)$, reaches its peak value. The frequency, $\nu(t_n)$, in each such signal burst, $i_n(t)$, represents a sample of the random process u(t). The burst duration, i.e. the width of $a_n(t)$ is given by the particle's transit time

$$\tau = 2w/u \qquad (4)$$

where 2w is the width of the probe volume along the particle trajectory. The finite transit time, τ, gives rise to the transit time broadening $\Delta_s\nu \sim 1/\tau$ (4,5,6) of the signal spectrum.

The Doppler bursts, i.e. the velocity samples, are not equally spaced in time, but occur at random times t_n whenever a scattering particle crosses the optical probe volume. As long as the time intervals between subsequent samples

$$\Delta t = t_{n+1} - t_n \leq \tau \; , \qquad (5)$$

in other words for heavy seeding, the individual bursts overlap. The signal envelope, a(t), becomes a continuous random function and the Doppler signal is quasi-continuous in the sense that the probability $P(a(t) < a_{th})$ for a signal envelope a(t) smaller than a preset threshold level $a_{th} \cong 0$ of the signal processor is negligible:

$$P(a(t) < a_{th}) \cong 0 \qquad (6)$$

Furthermore, it has been extensively shown (6), that in the case where many particles with random positions simultaneously traverse the probe volume, there are additional sources of broadening which contribute to the total spectral width of the signal. Especially, the phase fluctuations (6) due to the relative motion of the particles simulate random velocity fluctuations of the fluid even for constant laminar flows. All these broadening effects are of major importance for measurements in low turbulence intensity flows. They set the lower limit for the velocity fluctuations of the flowing medium that can be resolved (see Figure 8 of (6)). Since in this paper high turbulence intensity is of interest only, we may, for the sake of simplicity, neglect the broadening effects mentioned above and interpret the time - dependent signal frequency, $\nu(t)$, as if it was only reflecting the time - dependent velocity component, u(t), at the geometrical center of the probe volume. In this case the temporal resolution mainly depends on the design parameters of the signal processor.

For unseeded flows however the particle concentration is normally such, that the individual

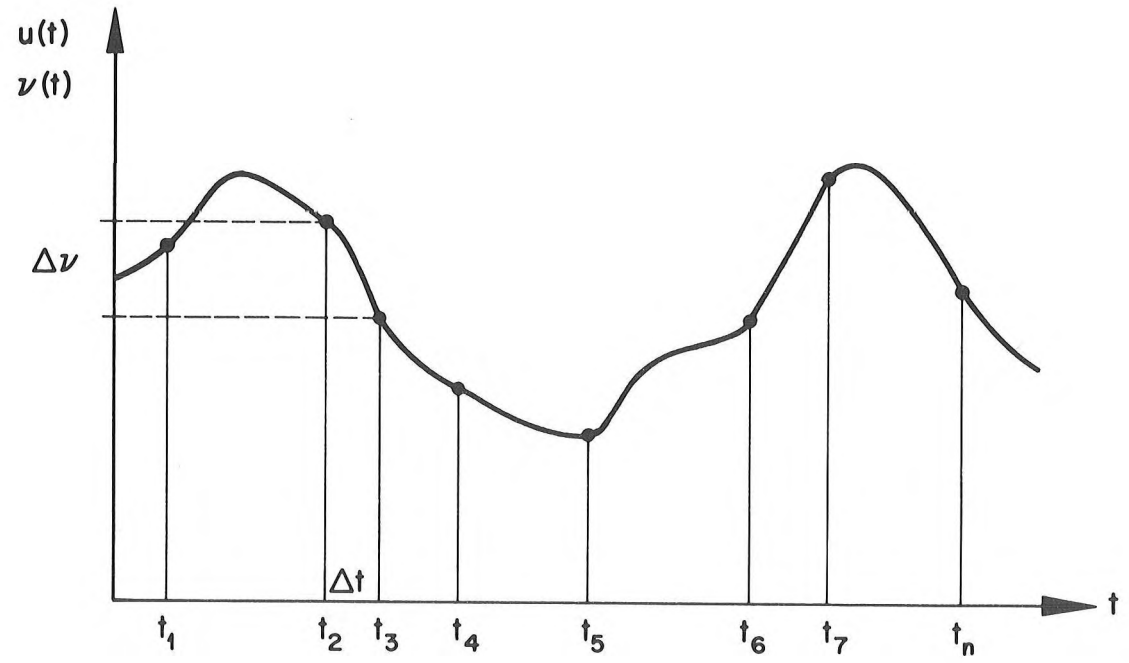

Figure 1. Flow velocity, u(t), or Doppler frequency, $\nu(t)$, randomly sampled at times, t_n, by scattering particles.

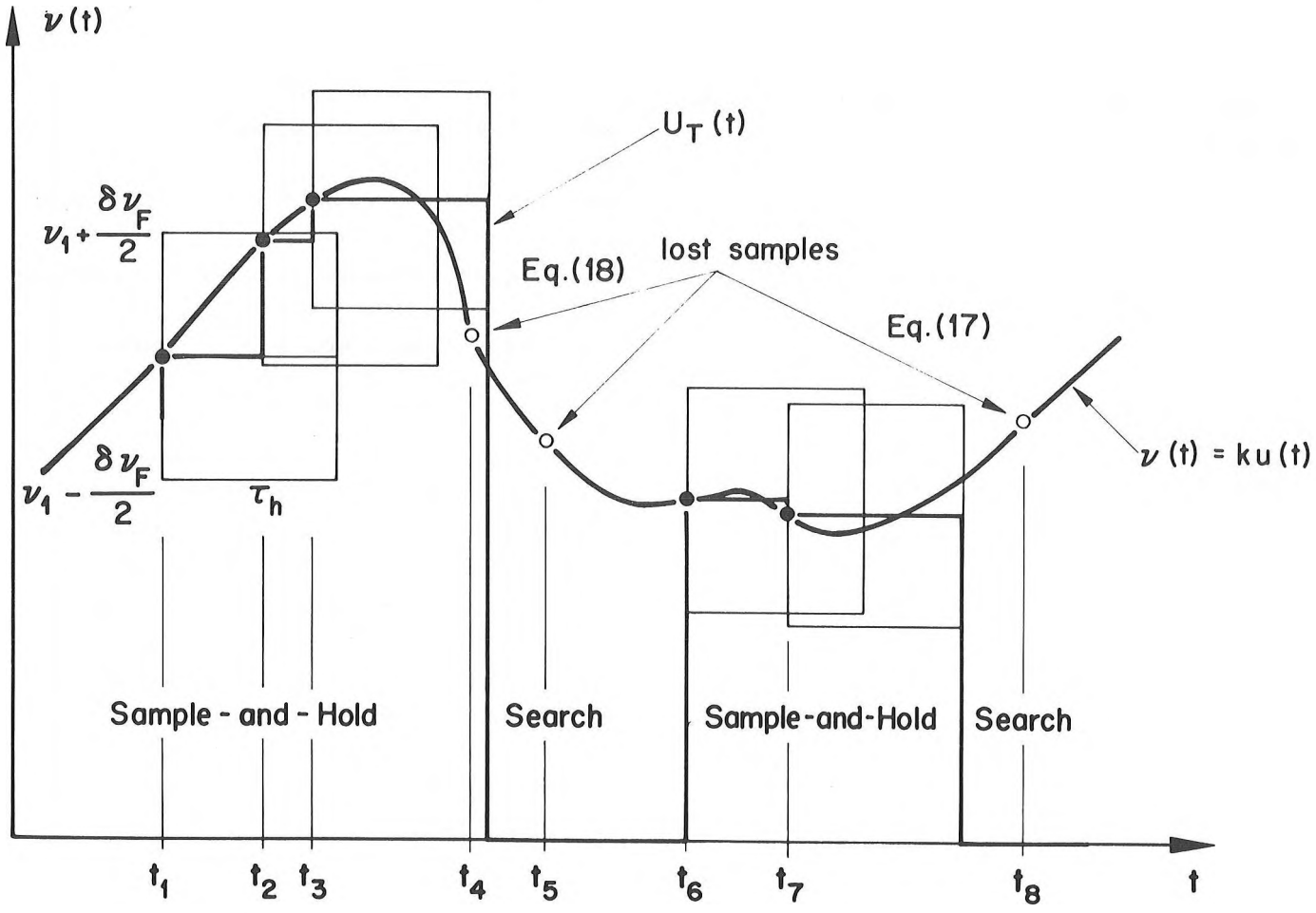

Figure 2. Staircase approximation of continuous velocity-time function, u(t), and measurement interruption (search) due to violation of sampling theorem.

Doppler bursts do not overlap:

$$\Delta t > \tau \tag{7}$$

The Doppler signal flow is therefore discontinuous in time and discrete velocity samples

$$u_n = u(t_n) = k^{-1}\, \nu(t_n) \tag{8}$$

are obtained.

Obviously, the random arrival of Doppler bursts, $i_n(t)$, is due to the random spatial distribution of scattering particles within the flow medium. The sample rate, Λ, depends on the particle concentration, C, and the time-dependent velocity, u(t):

$$\Lambda(t) = F\, C\, u(t) = \pi w_x w_z\, C\, u_y(t)\ . \tag{9}$$

F denotes the cross-section of the probe volume orthogonal to the flow velocity, u(t). For a velocity component, $u_y(t)$, in the y-direction, F is given by the semi-axes w_x and w_z of the ellipsoidal probe volume (4).

Since the samples can be assumed to be statistically independent they obey a Poisson distribution:

$$p(m,T) = \frac{(\overline{\Lambda}T)^m}{m!}\, e^{-\overline{\Lambda}T}\ . \tag{10}$$

p(m,T) is the probability that m samples occur during the time interval T for a process with mean sample rate $\overline{\Lambda}$, where $\overline{\Lambda}$ is given by the time-average

$$\overline{\Lambda}(t,T) = \frac{1}{T} \int_t^{t+T} \Lambda(t')\, dt' = \frac{FC}{T} \int_t^{t+T} u(t')dt'. \tag{11}$$

Assuming that the velocity, u(t), does not considerably change during the time interval, T, the approximation $\overline{\Lambda}(t,T) = \Lambda(t)$ is permissible. Hence, the probability distribution for the time intervals $\Delta t = t_{n+1} - t_n$ between subsequent samples is easily derived from the Poisson distribution. This leads to an exponential distribution (7):

$$p(\Delta t) = \Lambda e^{-\Lambda \Delta t}, \tag{12}$$

yielding a mean time interval

$$\overline{\Delta t} = 1/\Lambda\ . \tag{13}$$

Since the random distribution of velocity samples is analytically identical to the photon counting distribution for fluctuating light intensities a general solution to this problem can be found in a quantum optical textbook (8).

Due to the discontinuous information flow ($\Delta t > \tau$) the temporal resolution with which a velocity time function u(t) can be reconstructed essentially depends on the particle concentration in the sense that the sample rate, Λ, as given in Equation 9, has to satisfy the sampling theorem (1) and is therefore related to the turbulence bandwidth, B_{turb}, of the velocity, u(t), by

$$\Lambda > 2B_{turb}\ . \tag{14}$$

If, however, only an estimation of the power spectrum of u(t) is to be derived from randomly spaced samples, u_n (Equation 8), the sampling theorem, as stated above, must not necessarily be satisfied. This has been predicted theoretically (9) and recently verified experimentally (10).

It is evident from Equation 9 that in the case of an incompressible flow, i.e. time-independent particle concentration, C, the sample rate, $\Lambda(t)$, is linearly proportional to the flow velocity, u(t).

Thus the velocity samples, u_n, are <u>not</u> statistically independent of the velocity function to be sampled. Since the sample rate Λ increases with increasing velocity, the sample mean will always be biased towards higher velocities with respect to the mean of the continuous velocity u(t). As will be shown in a later section of the present paper, this has to be taken into account for the evaluation of statistical averages from single particle LDV data.

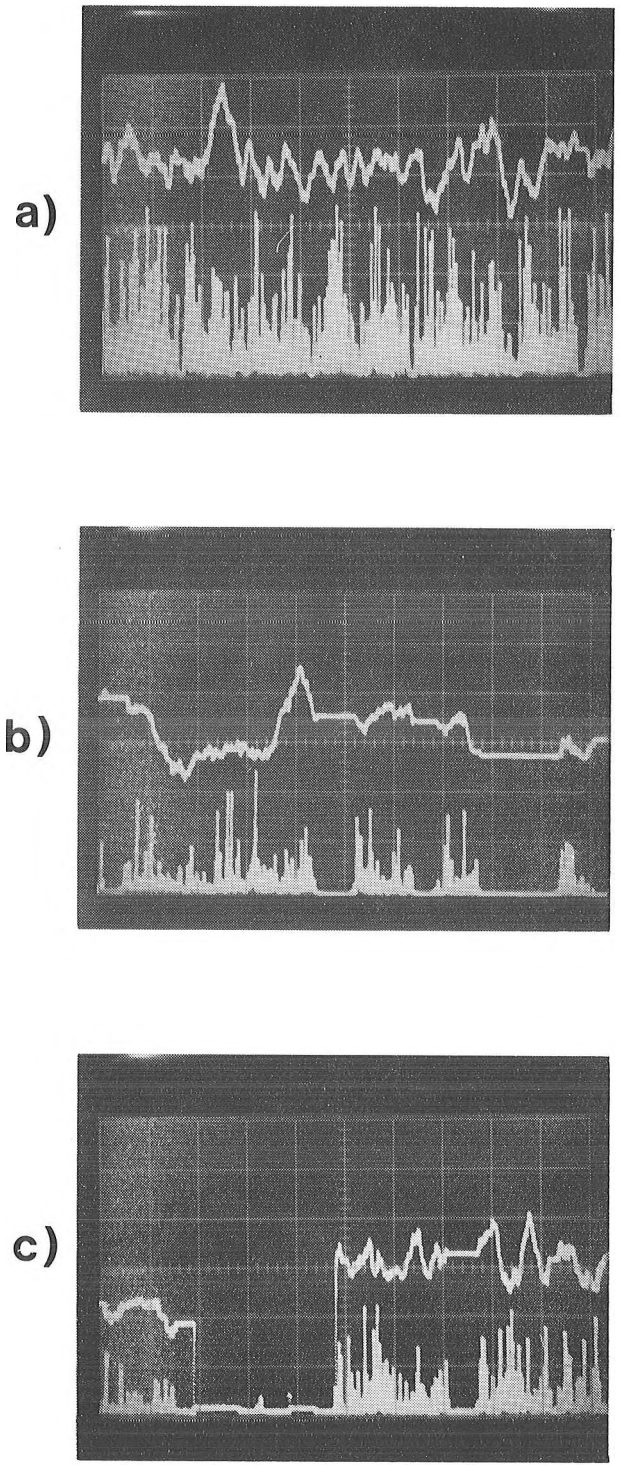

Figure 3. Response of a frequency tracker to turbulent flow for different particle concentrations. Upper traces: tracker output, $U_T(t)$, lower traces: envelopes, $a_n(t)$ of Doppler bursts.

a) quasicontinuous signal

b) signal drop out

c) signal drop out and new search.

lower traces are the envelopes, $a_n(t)$, of the Doppler bursts, $i_n(t)$, occurring within the IF-filter bandwidth, $\delta\nu_F$. The vertical scale of the lower traces equals 0.5 V/div and the threshold level, a_{th}, of the tracker is set to 0.1 div. In order that signal dropouts are clearly recognized on the oscilloscope screen, for explanatory reasons, the hold time, τ_h, is here set much longer than required by the sampling theorem of Equation 16, i.e. $\tau_h >> \tau_s$. For heavy seeding as shown in Figure 3a, Equation 6 is fulfilled ($\Delta t < \tau$) and the tracker follows satisfactorily the instantaneous flow velocity. If the particle concentration is reduced, signal dropout becomes obvious (Figure 3b) and the tracker remains in the hold mode during certain time intervals. For further reduced particle concentration the tracker output even drops to zero and the tracker has to search for the Doppler frequency anew (see also Figure 2).

It is evident from Figure 3 that reasonably correct values for mean velocity and turbulence intensity are only obtained in the case corresponding to Figure 3a. Only here the velocity fluctuations $\Delta\nu$ and the time intervals $\Delta t = t_{n+1} - t_n$ fulfill Equation 23. To correct the measured turbulence intensity for transit time and gradient broadening see References 6 and 15. For the situation shown in Figure 3b one might get a reasonably correct mean velocity by averaging, but the turbulence intensity as obtained from the rms value of the tracker output, will be smaller than its true value. Obviously the situation shown in Figure 3c (and Figure 2) is far beyond the point where a frequency tracker is able to operate satisfactorily. Here, neither mean velocity nor turbulence intensity can be determined reliably.

The conclusion is that tracking systems are only of limited use for investigations of turbulent flows. Seeding is in most cases necessary and has to be related to the temporal characteristics of the flow in order that Equation 5 or at least Equation 23 be fulfilled. Furthermore, the highest frequencies of the turbulence spectrum have to be within the response of the tracking loop.

DIGITAL FREQUENCY COUNTERS

An alternative method of frequency determination is the digital counting of the number, m_n, of signal periods, $T_d = 1/\nu$, during a preset time interval, $T_n < \tau$, of the n-th Doppler burst, $i_n(t)$ (frequency counting), or the counting of the time interval, T_n, equal to a preset number, m_n, of signal periods, T_d (period counting), (2,16). Both methods yield, for the averaged signal period,

$$\overline{T}_d \cong \overline{\nu}^{-1} = \frac{M_n T_c}{m_n} = (ku_n)^{-1} \qquad (24)$$

where M_n is the counter reading and T_c the period of the digital clock. Due to the digital uncertainty of $\pm$ 1 count in the counter reading, M_n, the following measurement uncertainty, δT_d, for a single Doppler burst is obtained:

$$\frac{\delta T_d}{\overline{T}_d} \cong \frac{\delta\nu}{\nu} = \pm \frac{1}{M_n} . \qquad (25)$$

The digital information of the counter reading may be converted into an analog signal (2) in order to obtain a staircase approximation of the velocity function u(t) (Figure 2).

For continuous Doppler signals ($\Delta t < \tau$) the system response time is ultimately limited by the period time T_d of one single Doppler cycle. For single burst signals ($\Delta t > \tau$) the basic limit for the temporal resolution is again given by the sampling theorem of Equation 16.

In contrast to the tracking receiver the gated zero crossing detector accepts any frequency sample, $\nu(t_n)$, within its total detection bandwidth, B, and, therefore the frequency change, $\Delta\nu$, (Equation 18 and Figure 2) between subsequent Doppler bursts is not limited to a small IF-filter bandwidth, $\delta\nu_F$. Therefore, counting systems are less problematic in turbulent flows than frequency trackers. However, in order that the staircase approximation be a reasonable reconstruction of the velocity function, u(t), the basic limitations as derived for the frequency tracker, have to be observed also.

The general application of this fast response system is somewhat hampered by the following facts:

Since the noise bandwidth of a gated zero crossing detector is equal to its detection bandwidth, B, noise rejection is rather poor. Therefore, Doppler signals with high SNR are demanded.

Second, for proper counting of the zero crossings a Doppler burst has to be a pure ac-signal, as given in Equation 3. Therefore, the Doppler signal of a real fringe system (4) must be filtered in order to completely remove the signal pedestal (17). This necessitates an automatic filter bank (2) or balanced optical detection (17).

Third, due to the digital counting with a finite clock time, T_c, zero crossing detectors have a rather low upper frequency limit. As an example the measurement accuracy for the commonly used 8-period-counter ($m_n = 8$) can be calculated from Equations 24 and 25. Even for a clock frequency as high as $\nu_c = 1/T_c = 100$ MHz, the maximum Doppler frequency is limited to $\nu \leq 8$ MHz in order to assure an accuracy of $\Delta\nu/\nu \leq 1\%$. This limits the application to low and medium range velocities.

SAMPLING TECHNIQUES

It has been shown so far that the reconstruction of the velocity-time function, u(t), from discrete frequency samples, $\nu(t_n)$, can be very problematic for frequency trackers and counting systems. Hence, the processing of this reconstructed velocity-time function, u(t), might lead to considerable errors for the evaluation of turbulence characteristics.

In turbulence research it is not the velocity function itself which is of primary interest but rather statistical averages such as mean velocity, turbulence intensity, etc. If the turbulent flow is stationary in the statistical sense, at least first-order averages can be determined from an arbitrary set of discrete velocity samples, u_n (Equation8), as well as from the velocity-time function, u(t), itself.

Therefore, appropriate sampling techniques can be used to investigate the statistical properties of turbulent flows, even in cases where the scattering particle concentration or the signal processor response time does not allow for proper reconstruction of the velocity-time function, u(t). The optimum sampling system, in the sense that it is able to transform the frequency of each Doppler burst, $i_n(t)$, into a velocity sample, u_n, whatever the particle concentration may be, is the gated zero crossing detector. Here, the natural sample rate, Λ, as given in Equation 9, is not reduced by any filter bandwidth, $\delta\nu_F$. However, due to the problems mentioned above, a novel sampling signal processor has been conceived and realized which is able to determine first-order statistical parameters of turbulent flows with high fluctuation frequencies and amplitudes even at very low scattering particle concentration.

SAMPLING FM WIDE-BAND DEMODULATOR

The properties of this sampling system are described extensively in a previous paper (3). This sampling system has recently been successfully used in flow research (18, 19). It consists essentially of a swept filter, e.g. a standard RF-spectrum analyzer and a storage oscilloscope. As shown in Figure 4 the swept filter periodically scans the frequency range of interest. When coincidence between the swept filter frequency, $\nu_F(t)$, and the frequency of a Doppler burst occurs, a frequency (velocity) sample, $\nu(t_n) = k\, u_n$, is taken and displayed on the oscilloscope. To reject noise the pulse discriminator accepts only Doppler bursts the amplitude, $a_n(t)$, of which exceeds a settable threshold level, a_{th} (3).

The theoretical limit for Doppler frequency changes, at which velocity samples can be recorded, is given by

$$(d\nu/dt)_{max} = (\delta\nu_F)^2 , \qquad (26)$$

where $\delta\nu_F$ is the bandwidth of the swept filter. For a frequency range of 100 MHz and a spectral resolution of 3% ($\delta\nu_F = 3$ MHz) Equation 26 yields $(d\nu/dt)_{max} = 9 \times 10^{12}\ s^{-2} = 9$ MHz/μs. Frequency

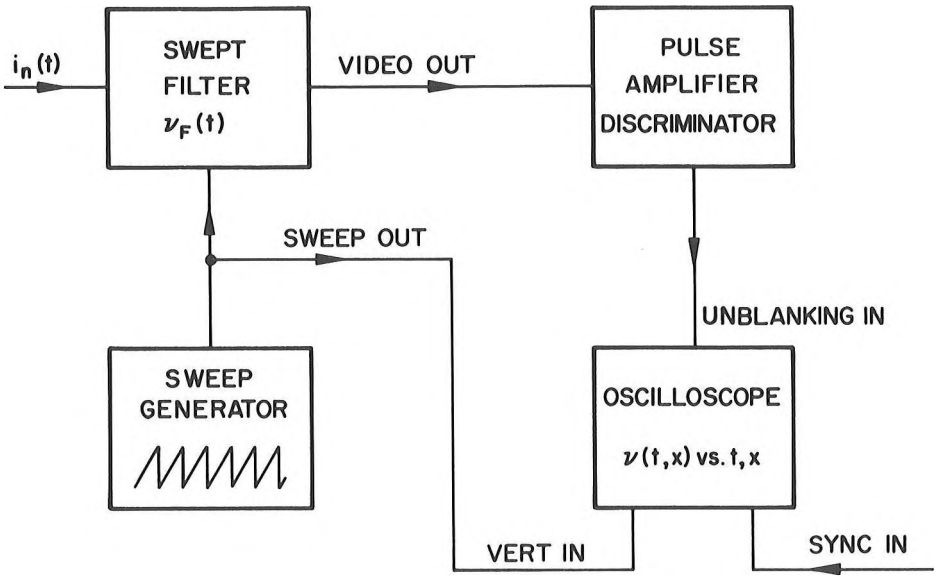

Figure 4. Block diagram of the sampling FM-discriminator.

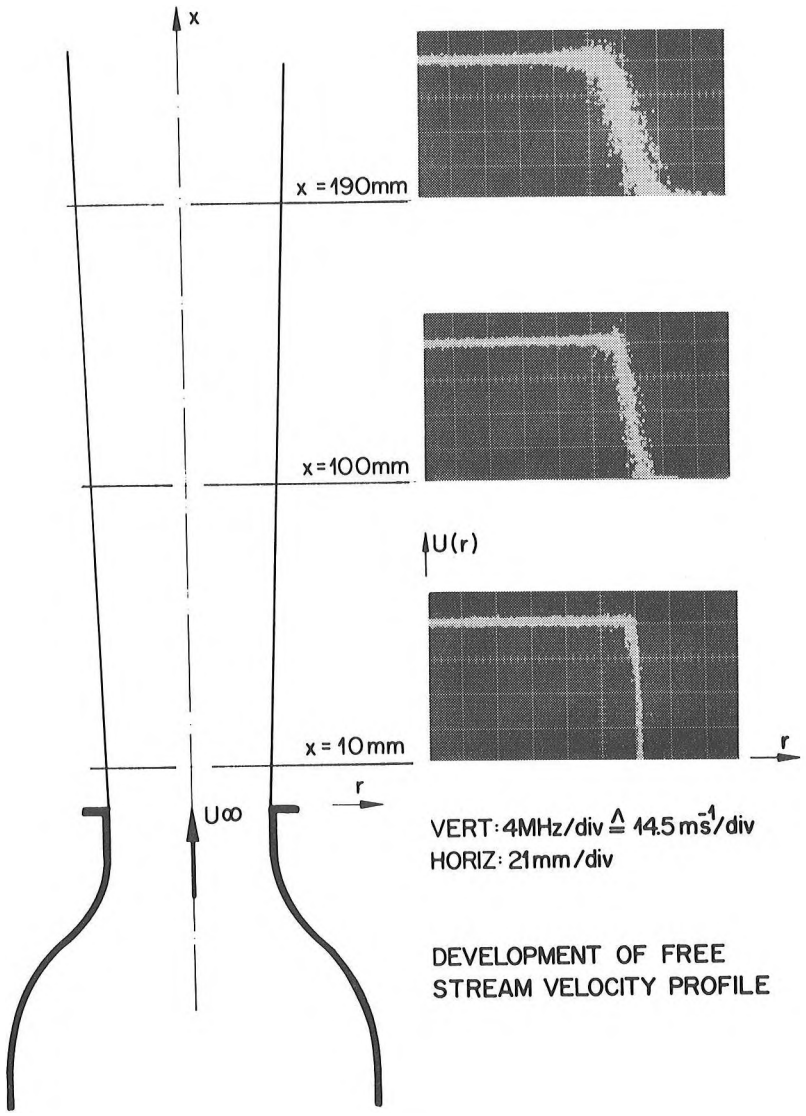

Figure 5. Velocity profiles in an air jet measured with the sampling FM-demodulator.

changes per time as high as $d\nu/dt = 10^{14}\ s^{-2}$ = 100 MHz/μs, which is 10 times the theoretical prediction, were resolved experimentally in the case of a good SNR (3). This means that for a typical LDV system constant of about k = 1 MHz/ms^{-1}, scattering particles having accelerations up to 100 ms^{-1}/μs = 10^8 ms^{-2} can produce a velocity sample.

The disadvantage of this system compared to zero crossing detectors consists in that the effective sample rate at the output of the swept filter is not only given by Equation 9 but also depends on the filter bandwidth, $\delta\nu_F$, and the total sweep range (detection bandwidth), B. Using Equations 9 and 11, the effective mean sample rate for the sampling FM demodulator is approximately given by

$$\bar{\Lambda}' = FC\bar{u}\,\frac{\delta\nu_F}{B}\,, \qquad (27)$$

where $\bar{u}$ denotes the mean velocity.

With the system sketched in Figure 4 a real-time display of the velocity samples, u_n, versus time or versus position of the probe volume is obtained directly on the storage screen of the oscilloscope. Examples of velocity profiles in an air jet measured with the sampling FM-demodulator, are shown in Figure 5. The free stream profile is slowly scanned at different distances downstream of the outlet of the nozzle. The horizontal deflection of the oscilloscope is proportional to the radial position r of the probe volume within the free stream and the vertical deflection corresponds to the velocity. In Figure 5 individual velocity samples are clearly recognized as distinct dots on the oscilloscope screen. The scatter of these sample points give a direct visualization of the turbulence at different positions. From these profiles the mean velocity, $\bar{u}(r)$, and the turbulence intensity, $\sigma_u(r)$, can be estimated. The accuracy is however limited due to the analog representation of the velocity data. Therefore, the sampling FM-demodulator depicted in Figure 4 has been extended as shown in Figure 6. This modified version essentially consists of the same parts as described in Figure 4. But in addition to the analog representation of the frequency samples, ν_n, on the oscilloscope, they are digitally processed in a multichannel analyzer in order to obtain the probability density function (PDF), $p^*(\nu)$, of the frequency samples, ν_n. This is performed by sampling the sweep voltage, which is proportional to the swept filter frequency, $\nu_F(t)$, at the times of coincidence between, $\nu_F(t)$, and the Doppler frequency with the appropriately delayed sampling pulses, $U_1(t)$. The delay time Δt yields a first order compensation for the finite spectral width $\Delta_s\nu \sim 1/\tau$ of the Doppler signal. After completion of a sufficient set of samples, ν_n, the data stored in the multichannel analyzer are fed into a computer for calculation of the statistical averages. Since the Doppler frequency is given by $\nu(t) = k\,u(t)$, the frequency PDF, $p(\nu)$, is identical with the PDF, $p(u)$, of the velocity, u(t).

As mentioned earlier (Equation 9), the velocity samples, $u_n = k^{-1}\,\nu_n$ - independent of whether they be taken with a zero crossing detector or a sampling FM-demodulator - are not statistically independent of the velocity function u(t), to be sampled. Therefore, the PDF, $p^*(u)$, of the velocity samples, u_n, is a biased sample distribution and does not lead to the correct statistical averages, as would be obtained from the PDF, p(u), of the velocity, u(t). However, since the relation between the sample rate, Λ (Equation 9), and the velocity, u(t), is known, p(u) can be determined from $p^*(u)$.

For a unidirectional flow, i.e. $u > 0$, $p^*(u)$ and p(u) are related by

$$p^*(u) = \frac{u}{\bar{u}}\,p(u), \quad \text{or} \quad p(u) = \frac{\bar{u}}{u}\,p^*(u) \qquad (28)$$

where the mean velocity $\bar{u}$ is obtained from $p^*(u)$ by

$$\frac{1}{\bar{u}} = \int \frac{p^*(u)}{u}\,du\,, \qquad (29)$$

using Equation 28 and the normalization condition for p(u).

From the PDF, p(u) (Equation 28), the first-order statistical properties of the turbulent flow can be calculated. Mean velocity, $\bar{u}$, turbulence intensity, σ_u, and turbulence degree, $\sigma_u/\bar{u}$, are given by the following equations:

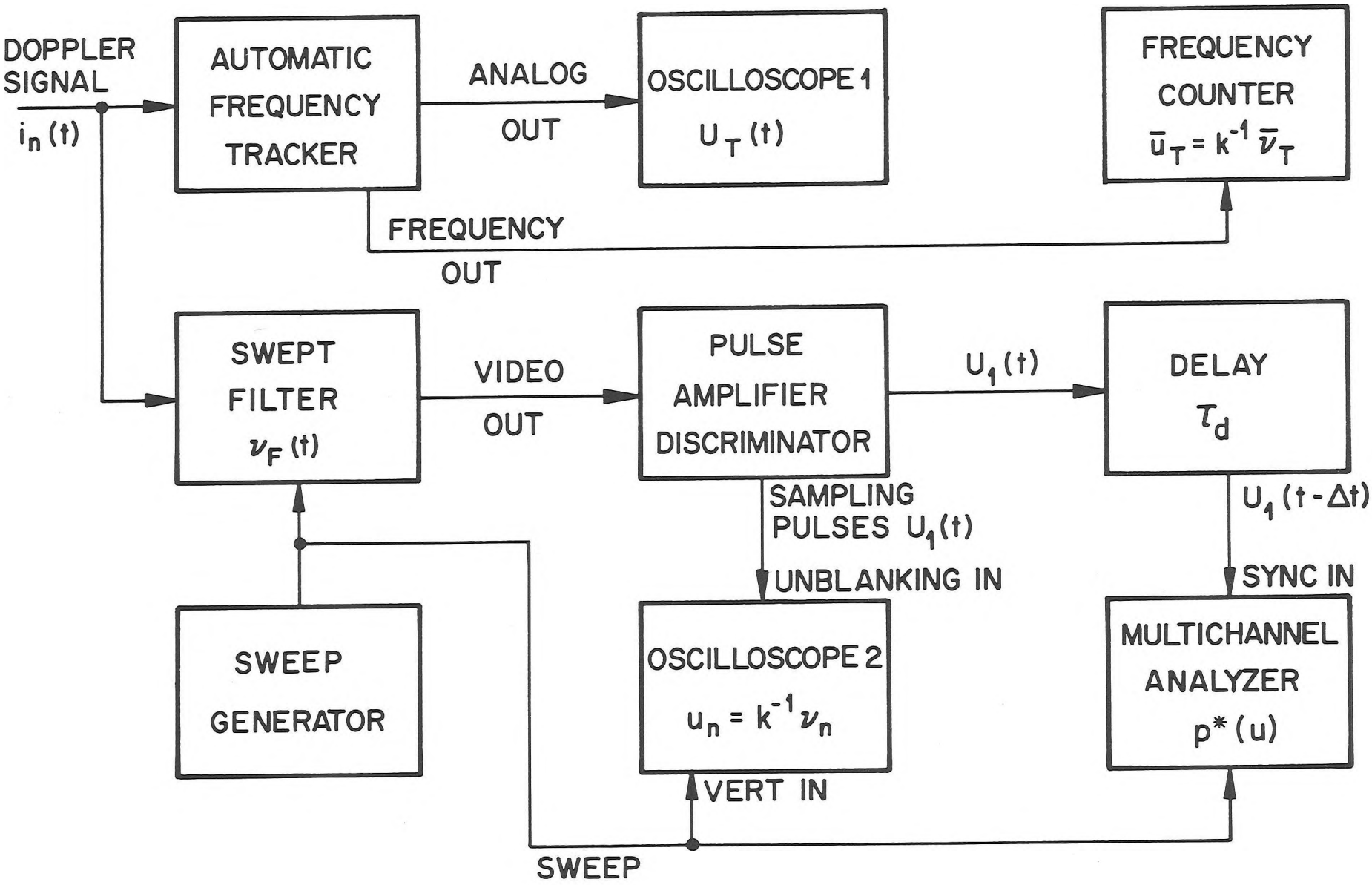

Figure 6. Block diagram of the measuring system consisting of a tracking receiver and a digital sampling FM-demodulator.

$$\bar{u} = \int u\, p\,(u)\, du$$

$$\sigma_u^2 = \int (u-\bar{u})^2\, p(u)\, du\ , \qquad (30)$$

with $\int p(u)\, du = 1$.

Instead of using Equations 28, 29 and 30 for calculating the unbiased mean $\bar{u}$ and variance σ_u^2 from the biased distribution $p^*(u)$, a first order approximation $\bar{u}^*$ and σ_u^* of $\bar{u}$ and σ_u, respectively, can be obtained directly from $p^*(u)$:

$$\bar{u}^* = \int u\, p^*(u)\, du$$

$$(\sigma_u^*)^2 = \int (u-\bar{u}^*)^2\, p^*(u) du\ , \qquad (31)$$

where $\bar{u}^*$ and $(\sigma_u^*)^2$ denote the sample mean and variance, respectively.

From Equations 31 and 28 the following expression is derived:

$$\bar{u}^* = \int u p^*(u)\, du = \frac{1}{\bar{u}} \int \bar{u}^2 p(u)\, du =$$

$$\bar{u}\,[1 + (\frac{\sigma_u}{\bar{u}})^2]. \qquad (32)$$

This shows that the relative error, $(\bar{u}^*-\bar{u})/\bar{u}$, between sample mean, $\bar{u}^*$, and true mean, $\bar{u}$, is simply given by the square of the turbulence degree, $(\sigma_u/\bar{u})^2$. In order that this error be smaller than 1% the turbulence degree must not exceed 10%.

Solving Equation 32 for $\bar{u}$ and substituting the unknown σ_u by the good approximation $\sigma_u^* \cong \sigma_u$, yields

$$\bar{u} = \bar{u}^*\, (1 + \sqrt{1 - 4(\sigma_u^*/\bar{u}^*)^2})/2\ , \qquad (33)$$

which allows the calculation of the mean velocity, $\bar{u}$, directly from the sample mean, $\bar{u}^*$, and variance, $(\sigma_u^*)^2$.

For unseeded flows the sample rate, Λ', is generally very small (Equation 27). Therefore, the minimum necessary measuring time, that guarantees a desired measurement error, should be known. The error of the experimentally measured PDF due to the finite total count number can be determined assuming uncorrelated fluctuations of the number of counts m_i in the i-th channel of the multichannel analyzer (20). The relative error of the probability, p_i, corresponding to the i-th channel is given by

$$\Delta p_i/p_i = \sqrt{m_i/M} = 1/\sqrt{p_i}\ , \qquad (34)$$

where $M = \Sigma\, m_i$ is the total number of counts.

The calculation of mean, variance and higher order moments from the sampling distribution, $p^*(u)$, is discussed in Reference 21. The relative rms error, $\Delta\bar{u}/\bar{u}$, of the mean velocity is given (21) as

$$\Delta\bar{u}/\bar{u} = (\sigma_u/\bar{u})/\sqrt{M}\ , \qquad (35)$$

where $\sigma_u/\bar{u}$ is the normalized standard deviation (turbulence degree) of the velocity. The rms error, $\Delta\sigma_u^2$, of the variance can be estimated from the variance, σ_u^2, assuming a normal distribution. The relative error $\Delta\sigma_u/\sigma_u$ is then found to be

$$\Delta\sigma_u/\sigma_u = \frac{1}{2}\, \Delta\sigma_u^2/\sigma_u^2 = 1/\sqrt{2M}\ . \qquad (36)$$

From Equations 35 and 36 the necessary total number of samples M to obtain a desired accuracy for the mean velocity and the turbulence degree can be calculated. It is advisable to choose the desired accuracy very carefully, because the necessary number of samples, M, increases as the square of the error reduction and so does also the measuring time, T_m. This time T_m can be estimated using Equation 27.

EXPERIMENTAL RESULTS

The optical part of the laser Doppler system used for the measurements is a fully integrated, modular optical head (22), operated in the forward-scattering fringe mode (4). The He-Ne laser in the optical head has 5 mW output power. The measurement angle is $2\chi = 16.7°$, which yields the system constant $k = 0.459\ \mathrm{MHz/ms^{-1}}$. The dimensions of the probe volume (4) are $2w_x \cong 2w_y = 75$ µm and $2w_z = 680$ µm.

The block diagram of the electronic signal processing system is shown in Figure 5. The Doppler signal, $i_n(t)$, is simultaneously fed into two different processing systems: the tracking receiver and the sampling FM-demodulator. This allows an experimental comparison of the performance of these two techniques for velocity measurements in unseeded turbulent flows.

The tracking receiver part consists of an automatic frequency tracker (12) with an analog output, $U_T(t)$, for the display of the frequency-time function and a frequency output for mean frequency measurements, $\bar{\nu}_T = k\bar{u}_T$, with a frequency counter. The frequency tracker has an automatic drop out holder and an automatic signal search (12).

Since both the automatic frequency tracker and the sampling FM-demodulator contain as basic part a swept filter, one can easily design an instrument (12) which can be operated in either of the two modes. This means that frequency tracker, sampling FM-demodulator, and even spectrum analyzer, are operational modes of the same Doppler signal processor rather than different instruments.

The first set of experiments was intended to check the performance of the described sampling FM-demodulator system under conditions where the flow velocity can be measured reliably with a frequency tracker. For this purpose highly stable Kármán vortices (23) in the wake of a tilted plate (2) were chosen. Figure 7a shows the velocity oscillations as measured with the frequency tracker in a water flow heavily seeded with artificial scattering particles. No signal drop-outs occurred and therefore the frequency tracker continuously followed the flow velocity u(t).

With a Hewlett Packard, Model 3721 A correlator, operated in the PDF-mode, the PDF, p(u), of the continuous tracker output, $U_T(t)$, (Figure 7a) was determined. The result is shown in Figure 7b. Numerical evaluation of mean velocity, $\bar{u}$, and standard deviation, σ_u, using Equation 30 yields $\bar{u} = 3.69 \times 10^{-2}$ ms^{-1} and $\sigma_u = 5.60 \times 10^{-3}$ ms^{-1}. Without changing the flow conditions, seeding was reduced such that only separated Doppler bursts at a low rate, Λ, were observed and the tracker immediately stopped working. Now, the PDF, p*(u), of the velocity samples, u_n, was measured with the digital version of the sampling FM-demodulator (Figure 6). The display of the multichannel analyzer is shown in Figure 7c. Note that the horizontal scales in the two figures 7b and 7c are different. Using Equation 31 the sample mean $\bar{u}^*$ and standard deviation σ_u^* were found to be $\bar{u}^* = 3.75 \times 10^{-2}$ ms^{-1} and $\sigma_u^* = 5.60 \times 10^{-3}$ ms^{-1}. Inserting these values in Equation 33 yields for the mean velocity $\bar{u} = 3.66 \times 10^{-2}$ ms^{-1}, which is in good agreement with the mean velocity as obtained above from the continuous velocity function, u(t) (tracker output $U_T(t)$).

The second set of experiments was intended to demonstrate the capability of the sampling system to measure the first order statistics of unseeded turbulent flows. For this purpose a turbulent pipe flow (24) was chosen. The flow medium was ordinary tap water. The pipe diameter was D = 2 R = 22.7 mm, the entrance length $\ell/D = 55$, and the Reynolds number $Re = \bar{u}_m D/\nu_{H_2O} = 8.2 \times 10^4$. The optical head of the LDV was mounted on a translation table to be able to scan the probe volume across the pipe diameter.

Two examples of sampled PDF, p*(u), are given in Figure 8. Figure 8a shows the expected bell-shaped PDF of the turbulent axial velocity component at the radial position r = 5.0 mm. At a position r = 10.2 mm, close to the pipe wall, an unexpected additional peak appears in the PDF (Figure 8b), which cannot be explained so far. The distributions shown in Figure 8 consist of about $M = 2 \times 10^4$ samples. From the PDF, p*(u), shown in Figure 8b, $\bar{u}^* = 3.16$ ms^{-1} and $\sigma_u^* = 0.49$ ms^{-1} are calculated by using Equation 31. Equation 35 then yields for the relative statistical error, due to the finite number of samples, $\Delta\bar{u}/\bar{u} \cong 1\%$, which is much lower than the other experimental errors.

Figure 8c shows the tracker output, $U_T(t)$, corresponding to the measurement point of Figure 8b (r = 10.2 mm). Comparison of both figures clearly demonstrates that the tracking system is not able to instantaneously measure the turbulent velocity. Due to the low concentration of the natural scattering particles in relation to the fast velocity changes, du/dt, the condition of Equation 23 for proper sampling of the velocity-time function, u(t), is not fulfilled. However, since the hold time, τ_h, (Equation 17) is set much longer than the mean time interval, $\overline{\Delta t}$ ($\tau_h >> \overline{\Delta t}$), tracking is not interrupted but the tracker is locked to the most probable Doppler bursts, i.e. to the peak of the PDF of

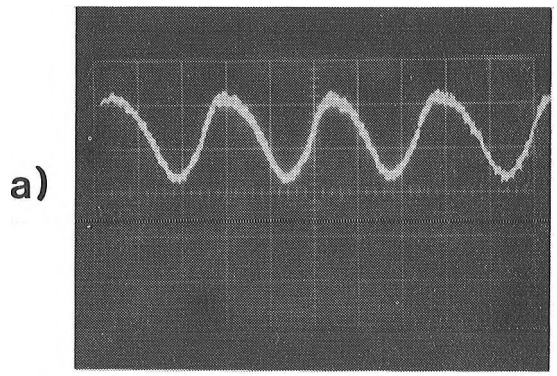

Figure 7. Periodic velocity variations of Karman vortices in the wake of a tilted plate

a) tracker analog output, $U_T(t)$: horiz. 0.2 s/div, vert. 4 kHz/div (k^{-1} = 2.17×10^{-3} ms^{-1}/kHz)

b) velocity probability density function (PDF), p(u), obtained from the continuous tracker output, $U_T(t)$: horiz. 2 kHz/div

c) velocity PDF, p*(u), obtained with the sampling FM-demodulator: horiz. 0.31 kHz/channel, center at 17.5 kHz, vert. 64 samples/div.

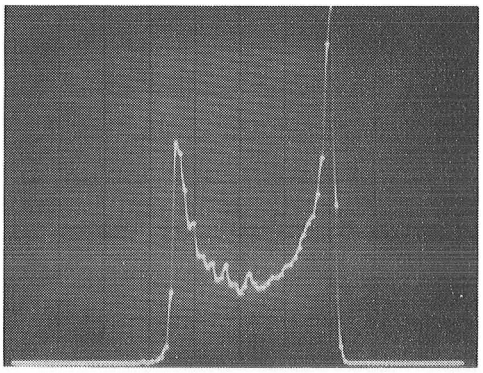

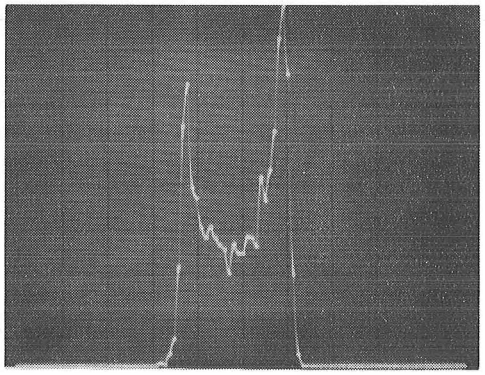

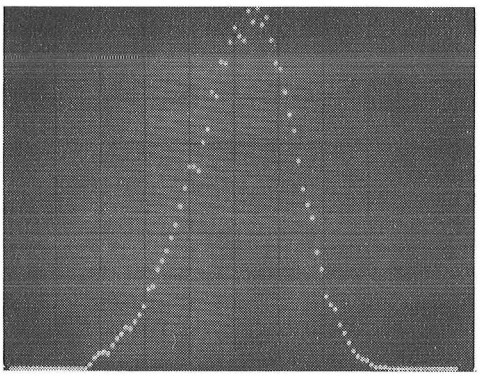

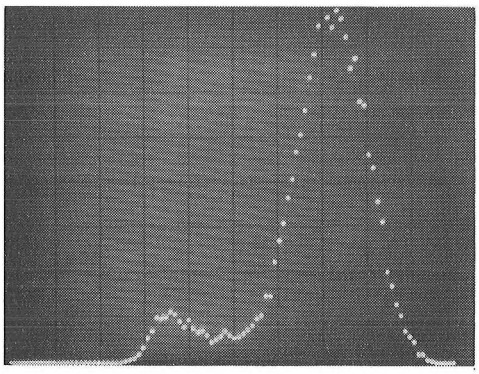

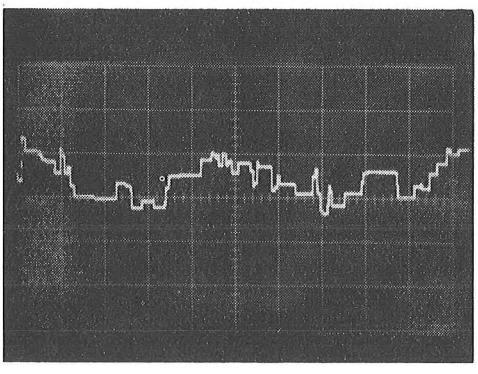

Figure 8. Velocity measurements in turbulent water pipe:

a) velocity probability distribution, p*(u), at r = 5.0 mm measured with the sampling FM-demodulator: horiz. 12.8 kHz/channel, center at 1.92 MHz, vert. 128 samples/div

b) p*(u) at r = 10.2 mm measured with the sampling FM-demodulator: horiz. 26 kHz/channel, center at 1.15 MHz, vert. 128 samples/div

c) analog output of tracker with drop-out holder for velocity measurement at r = 10.2 mm, horiz. 50 ms/div, vert. 40 kHz/div.

Figure 8a. Therefore, the tracker output, $U_T(t)$, as shown in Figure 8a is a random staircase function with relatively small fluctuations about the mean.

Hence, averaging this staircase function (or counting the frequency output, ν_T) during a sufficiently long time interval yields a zero order approximation of the mean velocity, $\bar{u}$. This means, that even in unseeded turbulent flows frequency trackers can be used, but only for the estimation of mean velocities triangles in Figure 9a). However, turbulence intensities obtained by measuring the rms value of the ac- part of this staircase function, $U_T(t)$, are drastically reduced with respect to the true values calculated from the PDF, $p^*(u)$.

By stepwise scanning the optical probe volume across the flow pipe, sampled velocity distributions, $p^*(u)$, for different radial positions, r, have been accumulated. Mean velocity, $\bar{u}^*$, and turbulence intensity, σ_u^*, are evaluated numerically by using Equation 31. The results are shown in the mean velocity profile, $\bar{u}^*(r)$, and the turbulence intensity profile, $\sigma_u^*(r)$, of Figures 9a and b, respectively. These first-order approximations could have been corrected by using Equation 33 in order to get $\bar{u}(r)$ instead of $\bar{u}^*(r)$. However, since the difference $(\bar{u}^*-\bar{u})/\bar{u}$ is less than 4% for any point of the profile and since the long term stability of the flow rate was of the same order, it was felt that a correction would have been meaningless. Furthermore, due to the short entrance length of $\ell/D = 55$, comparison with Laufer's data (24) would not have been possible, anyhow.

CONCLUSIONS

It has been shown (Figures 2 and 3) that the reconstruction of the velocity-time function, u(t), from discrete velocity samples can be very problematic for frequency trackers and to some extent also for zero-crossing detectors. Seeding with artificial scattering particles is of utmost importance. The particle concentration has to be related to the temporal characteristics of the flow (Equation 23). Therefore, tracking systems are only of limited use for investigations of turbulent flows.

It has been verified experimentally that the sampling FM-demodulator system is a powerful tool for turbulence measurements with laser Doppler velocimeters even in unseeded flows with very low particle concentrations. Since the sampling FM-demodulator is based upon a scanning RF-spectrum analyzer, frequency ranges up to the GHz-region can be covered. Moreover this sampling technique is practically independent of the upper frequency limit of the turbulence spectrum. The sampling FM-demodulator has been combined with a multichannel analyzer which stores the sampled velocity data in the form of a probability density function (PDF).

In a one-dimensional model it has been shown that for incompressible flows, i.e. time-independent scattering particle concentration, the velocity samples are <u>not</u> statistically independent of the velocity function to be sampled. Therefore, the sample mean, as derived from the PDF stored in the multichannel analyzer, is always biased towards higher velocities with respect to the true mean of the continuous velocity, u(t). Correction formulas for this velocity bias have been established and experimentally verified in Kármán vortices (Figure 7). The relative error between sample mean and true mean is simply given by the square of the turbulence degree.

Relations have been derived for the total number of velocity samples needed to assure results with a desired accuracy. The number of samples needed to determine the mean velocity increases with increasing turbulence degree, whereas the number of samples needed for calculating the turbulence intensity is independent of the flow.

Comparison of frequency trackers with sampling FM-demodulators show in general good agreement for mean velocity measurements. However, only sampling systems can measure reliably the turbulence intensity in unseeded flows.

ACKNOWLEDGMENT

The author is indebted to R. Dändliker for many fruitful and stimulating discussions. His constructive criticism was of great assistance during the course of this work.

SYMBOLS

$a_n(t)$	envelope of Doppler burst
a_{th}	threshold of signal processor
B	detection bandwidth, frequency range of signal processor, sweep range of swept filter

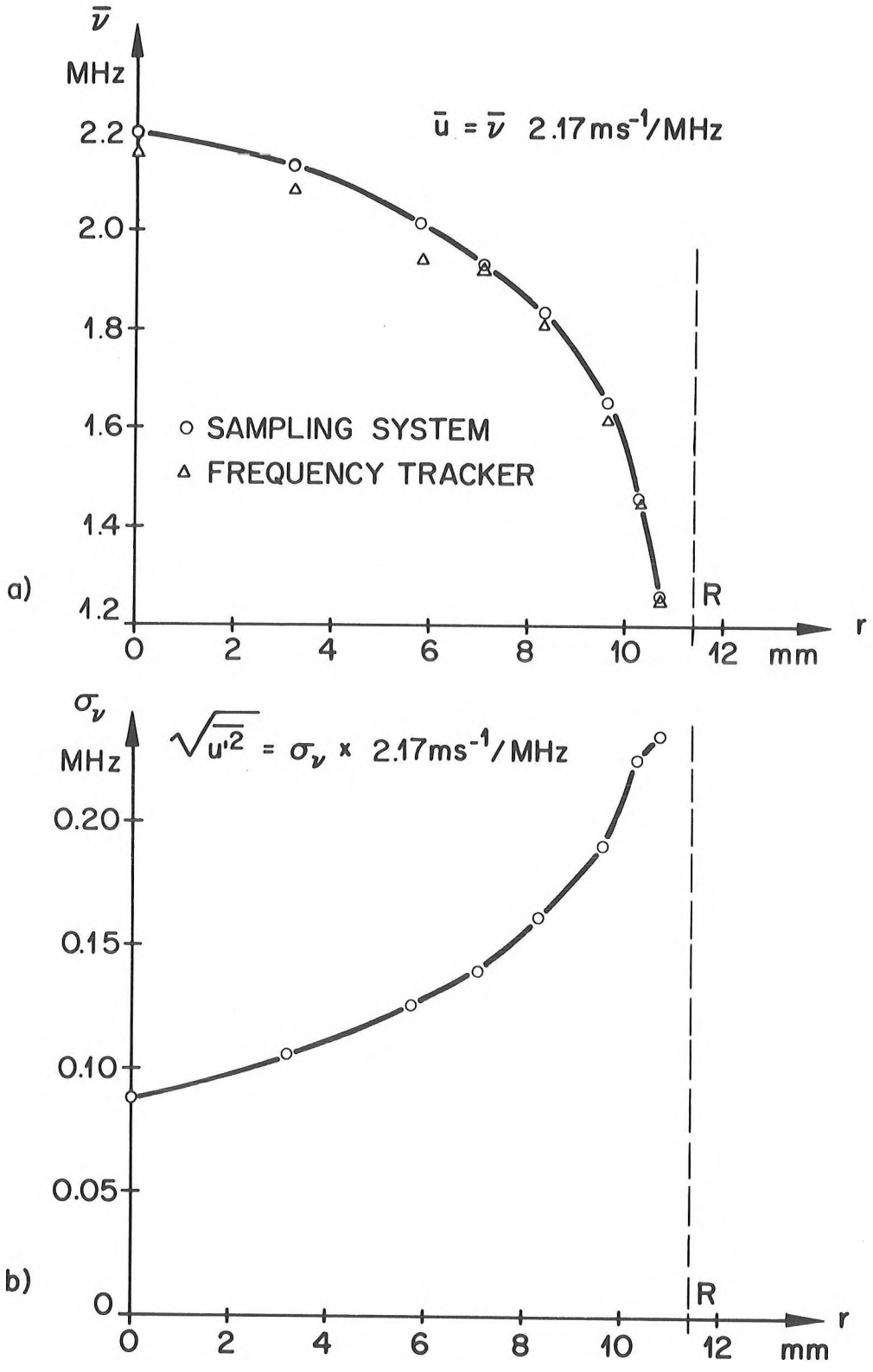

Figure 9. Statistical averages calculated from the probability density function, p*(u), for a turbulent pipe flow measured with the digital sampling FM-demodulator.

a) radial profile of the mean velocity, $\bar{u}$

b) radial profile of the turbulence intensity, $\sigma_u = \sqrt{\overline{u'^2}}$

SYMBOLS (cont.)

B_{turb}	turbulence bandwidth
C	concentration of scattering particles
D = 2R	diameter of flow pipe
$F=\pi w_x w_y$	probe volume cross-section orthogonal to flow
$i_n(t)$	Doppler signal of n-th particle
$\vec{k}$	sensitivity vector
$\lvert\vec{k}\rvert$	system constant, defined by Equation 2
l	entrance length
M	total number of samples in multichannel analyzer
M_n	counter reading for n-th particle
m_i	number of samples in i-th channel of multichannel analyzer
m_n	number of counted or preset signal periods
$P(a(t)<a_{th})$	probability that signal envelope, a(t), drops below threshold
$P(\Delta t<\tau_h)$	probability that time interval Δt is smaller than hold time, τ_h)
p_i	probability corresponding to i-th channel of multichannel analyzer
Δp_i	rms error of p_i
p(m,T)	Poisson probability density function (PDF)
$p(\Delta t)$	exponential PDF
p(u)	PDF of velocity function, u(t)
p*(u)	PDF of velocity samples, u_n
$p(\nu)$	PDF of frequency function, $\nu(t)$
$p^*(\nu)$	PDF of frequency samples, ν_n
r	radial position of probe volume
Re	Reynolds number
T_c	period of digital clock
T_d	Doppler period
$\overline{T}_d$	mean Doppler period averaged over T_n
T_n	measuring time of counter
t_n	time of occurrence of n-th Doppler burst
Δt	time interval between subsequent bursts
$\overline{\Delta t}$	mean time interval
$U_1(t)$	sampling pulses of sampling FM-demodulator
$U_T(t)$	output voltage of tracking system
u(t)	flow velocity, stationary random process
$u_k(t)$	velocity component along the direction of $\vec{k}$
u_n	velocity sample
$\overline{u}$	mean velocity
$\overline{u}^*$	velocity sample mean
Δu	rms error of mean velocity
w	half-width of probe volume along particle trajectory
w_x, w_y, w_z	semi-axes of elliptical probe volume
$\Lambda(t)$	time-dependent mean sample rate of Poisson Process
$\overline{\Lambda}(t,T)=\overline{\Lambda}$	time-averaged mean sample rate, $\Lambda(t)$, defined by Equation 11
$\overline{\Lambda}'$	effective mean sample rate as seen by sampling FM-demodulator
λ	laser wavelength in flow medium
$\nu(t)$	Doppler frequency
$\Delta\nu$	frequency change between subsequent bursts
$\Delta_s\nu$	transit time broadening
ν_c	frequency of digital clock
ν_F	center frequency of IF- or swept filter
$\delta\nu_F$	IF- or swept filter bandwidth, capture range
ν_n	frequency sample
$(d\nu/dt)_T$	slew rate of tracker
σ_u	turbulence intensity
σ^*_u	turbulence intensity derived from sample distribution, p*(u)
$\Delta\sigma_u$	rms error of turbulence intensity
τ	particle transit time
τ_d	delay time of sampling pulses, $U_1(t)$
τ_h	hold time of tracker
τ_ℓ	response time of tracking loop
τ_s	maximum sample interval
2χ	measurement angle in flow medium

REFERENCES

1. Shannon, C. E. and W. Weaver, The Mathematical Theory of Communication, Illinois Press, Urbana, pp. 86-87, 1964.

REFERENCES (cont.)

2. Iten, P. D., and J. Mastner, "A Laser Doppler Velocimeter Offering High Spatial and Temporal Resolution", presented at The Symposium on Flow - Its Measurement and Control in Science and Industry, May 10-14, 1971, Pittsburgh. Published in the Conference Proceedings, Instr. Soc. Am., Pittsburgh, 1974.

3. Iten, P. D., and R. Dändliker, "A Sampling FM Wide-Band Demodulator Useful for Laser Doppler Anemometry", Proc. IEEE, 60, 1470 (1972).

4. Eliasson, B., and R. Dändliker, "A Theoretical Analysis of Laser Doppler Flowmeters", Optica Acta, 21, 119, (1974).

5. Iten, P. D., B. Eliasson, and R. Dändliker, "Investigations and Improvement of Spectral and Spatial Resolution of a Laser Doppler Flowmeter", IEEE J. Quantum Electron, QE-7, 45, (1971).

6. George, W. K., and J. L. Lumley, "The Laser Doppler Velocimeter and its Application to the Measurements of Turbulence", J. Fluid Mech., 60, 321 (1973).

7. Papoulis, A., Probability, Random Variables, and Stochastic Processes, McGraw-Hill, New York, 556-557, 1965.

8. Klauder, J. R., and E. C. G. Sudarshan, Fundamentals of Quantum Optics, W. A. Benjamin, New York, pp. 16-23, 1968.

9. Shaw, L., "Spectral Estimates from Nonuniform Samples", IEEE Trans. on Audio and Electroacoustics, G-119, 24 (1971).

10. Mayo, W. T., Jr., S. Riter, and M. T. Shay, "An Introduction to the Estimation of Power Spectra from Single Particle LDV Data", presented at Workshop on Laser Doppler Anemometry, Oklahoma State University, Stillwater, Oklahoma, June 11-13, 1973.

11. Deighton, M. O., and A. E. Sayle, "An Electronic Tracker for the Continuous Measurement of Doppler Frequency from a Laser Anemometer", DISA Information, No. 12, 1971.

12. Mastner, J., and P. D. Iten, "A Fully Automatic High-Precision Laser Doppler Signal Processor", in preparation.

13. Kuo, B. C., Discrete-Data Control Systems, Prentice-Hall, Englewood Cliffs, N.J., pp. 1-5, 1970.

14. Ibid., pp. 26-29.

15. Berman, N. S., and J. W. Dunning, "Pipe Flow Measurements of Turbulence and Ambiguity Using Laser-Doppler Velocimetry", J. Fluid Mech., 61, 289 (1973).

16. Brayton, D. B., H. T. Kalb, and F. L. Grosswy, "Two Component Dual-Scatter LDV with Frequency Burst Signal Readout", Appl. Opt., 12, 1145 (1973).

17. Goethert, W. H., "Balanced Detection for the Dual Scatter Laser Doppler Velocimeter", Tech. Rep. AECD-TR-71-70, June 1971.

18. Simpson, R. L., J. H. Strickland, and P. W. Barr, "Features of a Separating Turbulent Boundary Layer as Revealed by Laser and Hot-Film Anemometry", presented at Symposium on Turbulence in Liquids, University of Missouri, Rolla, September 10-12, 1973.

19. Sullivan, J. P., and S. Ezekiel, "Two-Component LDV for Periodic Flow Field", to appear in J. Physics E.

20. Arecchi, F. T., A. Berné, A. Sona, and P. Burlamacchi, "Photocount Distributions and Field Statistics", IEEE J. Quantum Electron., QE-2, 341 (1966).

21. Cramér, H., Mathematical Methods of Statistics, University Press, Princeton, 341-352, 1966.

22. Iten, P. D., "An Integrated, Modular Laser Doppler Velocimeter", in preparation.

23. Schlichting, H., Grenzschicht-Theorie, G. Braun, Karlsruhe, 5th ed., pp. 28-32, 1965.

24. Laufer, J., "The Structure of Turbulence in Fully Developed Pipe Flow", NACA TR 1174, 1954.

DISCUSSION

J. H. Whitelaw, Imperial College: I distrust your statement about cleanliness of Swiss water. Is it possible that you had a finite and sizeable discrimination level built into the tracker system?

Iten: You always have a discrimination level.

Whitelaw: I agree, for instance, if you use the two trackers which we've had available to us recently, the Disa tracker or the Chemies Consultant tracker in water flows, one will give a dropout of around 2% and the other one of around 80%. I was wondering if it's that that makes your signal look discontinuous in your water flow?

H. M. Nagib, Illinois Institute of Technology: My question deals with your counting system. I think it's interesting to find out what kind of frequency response you can get out of it; how fast for example can we follow this?

Iten: I think you can probably track it a lot faster than the particles can follow it. It's generally the particles that are going to cause the biggest trouble, particularly in air kinds of flow.